MCB
Journals.ASM.org

O_2 Regulates Skeletal Muscle Progenitor Differentiation through Phosphatidylinositol 3-Kinase/AKT Signaling

Amar J. Majmundar,[a,b] Nicolas Skuli,[a,b] Rickson C. Mesquita,[d] Meeri N. Kim,[d] Arjun G. Yodh,[d] Michelle Nguyen-McCarty,[a,b] and M. Celeste Simon[a,b,c]

Abramson Family Cancer Research Institute,[a] Department of Cell and Developmental Biology,[b] and Howard Hughes Medical Institute,[c] Perelman School of Medicine at the University of Pennsylvania, Philadelphia, Pennsylvania, USA, and Department of Physics and Astronomy, University of Pennsylvania, Philadelphia, Pennsylvania, USA[d]

Skeletal muscle stem/progenitor cells, which give rise to terminally differentiated muscle, represent potential therapies for skeletal muscle diseases. Delineating the factors regulating these precursors will facilitate their reliable application in human muscle repair. During embryonic development and adult regeneration, skeletal muscle progenitors reside in low-O_2 environments before local blood vessels and differentiated muscle form. Prior studies established that low O_2 levels (hypoxia) maintained muscle progenitors in an undifferentiated state *in vitro*, although it remained unclear if progenitor differentiation was coordinated with O_2 availability *in vivo*. In addition, the molecular signals linking O_2 to progenitor differentiation are incompletely understood. Here we show that the muscle differentiation program is repressed by hypoxia *in vitro* and ischemia *in vivo*. Surprisingly, hypoxia can significantly impair differentiation in the absence of hypoxia-inducible factors (HIFs), the primary developmental effectors of O_2. In order to maintain the undifferentiated state, low O_2 levels block the phosphatidylinositol 3-kinase/AKT pathway in a predominantly HIF1α-independent fashion. O_2 deprivation affects AKT activity by reducing insulin-like growth factor I receptor sensitivity to growth factors. We conclude that AKT represents a key molecular link between O_2 and skeletal muscle differentiation.

Skeletal muscle damage or loss arises in a range of diseases, including inherited muscular dystrophies, critical limb ischemia in peripheral arterial disease (PAD), and aging-related sarcopenia (4, 10, 22, 26, 33). Weakened and aberrant muscles contribute significantly to the morbidity and mortality of patients suffering from these illnesses (4, 10, 22, 26, 33). Skeletal muscle stem/progenitor cells, which give rise to embryonic and adult muscle (32, 34), represent potential therapies for human skeletal muscle disease (22, 57). Delineating the pathways controlling the maintenance and differentiation of these precursors will facilitate their reliable application in muscle repair (22, 57).

In adult mammals, skeletal muscle stem cells—"satellite cells"—reside in a niche enveloped by differentiated muscle fibers and a layer of basement membrane. Quiescent satellite cells, expressing the transcription factor PAX7, become activated after muscle injury and terminally differentiate into new multinucleated skeletal muscle fibers (32, 34). These processes depend on several transcription factors known as muscle regulatory factors, or MRFs: MYF5, MYOD, and myogenin (Fig. 1A) (32, 34). MYF5 and MYOD are coexpressed with PAX7 in activated satellite cells but possess distinct functional roles (Fig. 1A) (32, 34). While MYF5 is important for muscle progenitor proliferation, MYOD is required for subsequent differentiation of these precursors (Fig. 1A) (32, 34). MYOD and its target, myogenin, stimulate terminal differentiation through the activation of genes expressed in mature muscle (e.g., *Myosin heavy chain*) (32, 34).

Skeletal muscle differentiation, or myogenesis, is tightly regulated and responds to environmental cues (32, 34). For example, insulin and insulin-like growth factors (IGFs) can act upon cultured muscle progenitors, termed myoblasts, and stimulate their terminal differentiation (18). In agreement with these findings, IGF-I has been shown to promote embryonic skeletal muscle development (36) and adult muscle regeneration *in vivo* (48). A key pathway activated by insulin and IGFs is phosphatidylinositol 3-kinase (PI3K)/mammalian target of rapamycin complex 2 (mTORC2)/AKT. These molecules are required downstream of insulin/IGFs for muscle differentiation *in vitro* (13, 14, 28, 29, 41, 59–62). For example, it was recently demonstrated that the mTORC2 component RICTOR regulates terminal myoblast differentiation upstream of AKT (54). AKT, furthermore, has been shown to promote embryonic muscle development and adult regeneration *in vivo* (44, 47).

Skeletal muscle progenitors also respond to the availability of local nutrients, such as glucose (20) and molecular oxygen (O_2) (15, 25, 51, 64). In fact, skeletal muscle is marked by reduced O_2 availability, or hypoxia, during both development and disease. Embryonic somites, where early skeletal muscle progenitors reside, exhibit increased expression of hypoxic markers (e.g., hypoxia inducible factor 1α [HIF1α]) prior to the formation of local blood vessels and embryonic muscle (49, 50). In addition, adult skeletal muscle exhibits severe pathological hypoxia in peripheral arterial disease (4, 7, 24, 26, 33, 45). Hind limb ischemia, or insufficient blood supply, acutely leads to tissue damage in mouse models of this disease (7, 24, 45). In otherwise-healthy animals, skeletal muscle progenitors as well as injured muscle fibers experience O_2 and nutrient deprivation until neovascularization restores perfusion to the tissue (7, 24, 45). As blood flow returns,

Received 24 June 2011 Returned for modification 6 August 2011
Accepted 9 October 2011
Published ahead of print 17 October 2011
Address correspondence to M. Celeste Simon, celeste2@mail.med.upenn.edu.
Copyright © 2012, American Society for Microbiology. All Rights Reserved.
doi:10.1128/MCB.05857-11

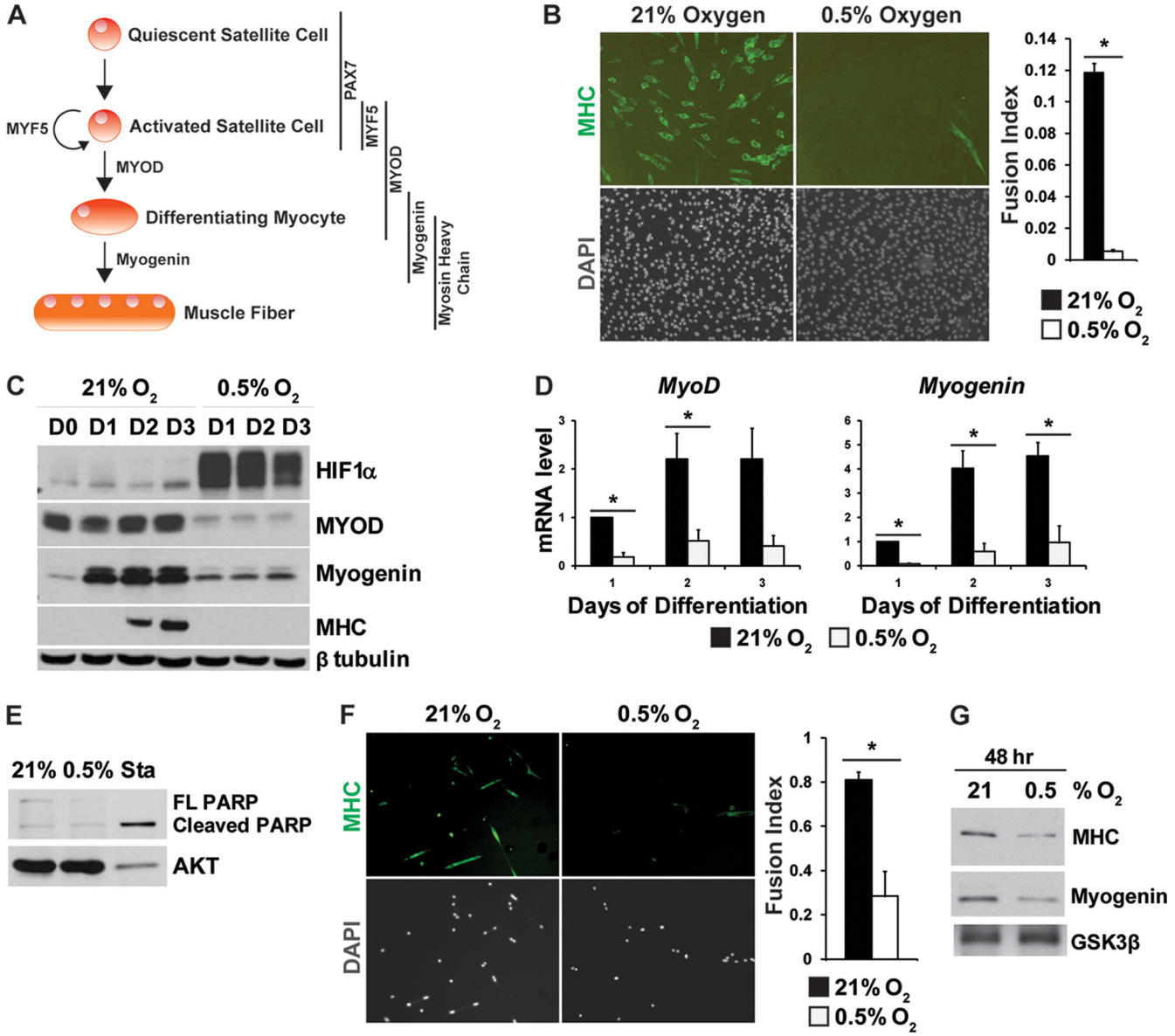

FIG 1 Low O_2 availability represses skeletal muscle progenitor differentiation *in vitro*. (A) Skeletal muscle progenitor differentiation model. Lineage markers are shown adjacent to the appropriate stages. (B) C2C12 myoblasts were differentiated for 96 h in 21% or 0.5% O_2. IF for MHC was performed. The fusion index was calculated. (C) HIF1α, MYOD, myogenin, MHC, and β-tubulin protein expression levels were detected in lysates from C2C12 cells cultured in 21% or 0.5% O_2 after 1, 2, and 3 days of differentiation. D0, day 0; D1, day 1; D2, day 2; D3, day 3. (D) C2C12 myoblasts were cultured as for panel C, and the mRNA expression levels of muscle regulatory factors *MyoD* and *Myogenin* were assayed by qRT-PCR using total RNA isolated from myoblast cultures. Averages of 3 independent experiments are shown. (E) Protein expression of PARP and AKT was detected in lysates from C2C12 myoblasts after 48 h of differentiation in 21% O_2, 0.5% O_2, or in the presence of the cytotoxic agent staurosporine (Sta). (F) Primary mouse myoblasts were differentiated for 48 h in 21% or 0.5% O_2. IF for MHC was performed. The fusion index was calculated. (G) Myogenin, MHC, and GSK3β protein expression levels were determined in lysates derived from primary myoblast cultures, as described for panel F. *, statistically significant difference based on Student's *t* test ($P < 0.05$).

newly generated fibers reconstitute affected muscle groups (7, 24, 45). Thus, in both embryonic development and adult regeneration, skeletal muscle stem/progenitor cells reside in a hypoxic microenvironment before the formation of local blood vessels and terminally differentiated muscle (7, 24, 45, 49, 50). In severe cases of PAD, however, vascular insufficiency and muscle damage can persist chronically (4, 26, 33).

O_2 may exert a developmental function in these contexts, for low-O_2 conditions are known to maintain skeletal myoblasts in an undifferentiated state *in vitro* (15, 25, 51, 64). This suggests that in the hypoxic microenvironment of developing or regenerating skeletal muscle, O_2-dependent pathways may constrain progenitor differentiation until there is ample blood supply, thereby conserving the stem/progenitor pool for appropriate circumstances for growth. However, this has not been formally tested *in vivo*.

While it is established that O_2 regulates myoblast differentiation, the molecular mechanisms are incompletely understood. In other tissues, HIFs represent the principal developmental effectors of O_2 availability (55). These transcription factors are comprised of an O_2-labile α-subunit and O_2-independent β-subunit

(37). Under hypoxic conditions, the two biologically relevant α-subunits, HIF1α and HIF2α, are stabilized and form dimers with HIF1β to activate the expression of numerous genes (37). The role of the HIFs in myogenesis has been controversial. In one study, ectopic HIF1α did not affect myoblast differentiation under ambient O_2 conditions (64). Another claimed that hypoxia inhibited muscle progenitor differentiation through a novel complex between HIF1α and NOTCH (25). However, neither report showed if endogenous HIFα was essential for the effects of hypoxia on myogenesis (25, 64).

In the present study, we employed animal and cell culture models to determine if O_2 can influence the myogenic program *in vivo* and to delineate which factors modulate skeletal muscle progenitors in response to low O_2. We show that low O_2 inhibits muscle progenitor differentiation and myogenic regulatory factor expression *in vitro*. In a murine model of PAD, MRF expression was similarly affected by ischemia *in vivo*. We then pursued the mechanism(s) linking O_2 to muscle differentiation. Surprisingly, while HIF1α deficiency had modest effects on myoblast differentiation, hypoxia can significantly modulate progenitor differentiation in the absence of HIF1α. We determined that hypoxia regulates muscle differentiation through predominantly HIF1α-independent effects on PI3K/mTORC2/AKT signaling. Low O_2 levels block PI3K/AKT signaling by reducing IGF-I receptor (IGF-IR) sensitivity to growth factors, and restoration of PI3K/AKT activity is sufficient to rescue myoblast differentiation. These findings suggest that HIF-independent factors may regulate the capacity of progenitors to repair skeletal muscle in settings of hypoxic/ischemic injury.

MATERIALS AND METHODS

Cell culture. C2C12 myoblasts (CRL-1772; ATCC) were propagated in 20% fetal bovine serum (FBS) in Dulbecco's modified Eagle's medium (DMEM). To evaluate differentiation, myoblasts were grown to 80 to 90% confluence and switched to 2% horse serum in DMEM.

Primary mouse myoblasts were isolated from gastrocnemius muscles of 8- to 12-week-old C57BL/6 mice as described in reference 56. Briefly, calf muscles were dissected, minced, and digested with 0.2% type II collagenase. Fibers were subsequently triturated, washed, and further digested in 1% dispase–0.05% type II collagenase. Satellite cells were displaced from fibers by triturating through an 18-gauge needle. Cells were further washed, decanted through a 40-μm strainer, and plated onto collagen-coated dishes. Primary cells were expanded in 20% FBS and 10 ng/ml recombinant human fibroblast growth factor (Promega) in Ham's F-10 for 7 to 9 days. For differentiation assays, 7.5×10^3 cells were plated in a 24-well plate overnight, and the medium was changed to 5% horse serum in DMEM.

Low-oxygen conditions were achieved in a Ruskinn in vivo$_2$ 400 work station. The following inhibitors were used to modulate PI3K and mTORC activities: 10 μM LY294002, 40 nM rapamycin,, and 250 nM Torin1 (gift from the D. Sabatini laboratory). Recombinant IGF-I and NOTCH ligand fusion protein Fc-JAG1 were purchased from R&D systems. γ-Secretase inhibitors DAPT (10 μM) and L-685,458 (1 μM) were purchased from Sigma-Aldrich.

Virus preparation. For shRNA-mediated knockdown of *Hif1α* and *Pten*, lentiviral particles bearing pLKO.1 shRNA plasmids were generated in HEK-293T cells. 293T cells were transfected overnight with pLKO.1 empty vector, nonspecific shRNA, or target-specific shRNA and viral packaging plasmids, according to the Fugene reagent protocol (Roche). The following shRNA pLKO.1 plasmids were employed: pLKO.1 empty (Addgene 8543), pLKO.1 scrambled shRNA (Addgene 1864), pLKO.1 *Hif1α* shRNA (TRCN0000054451), pLKO.1 *Pten* shRNA (TRCN0000028991), G protein of vesicular stomatitis virus (VSV-G), pMDLG, pRSV-rev. Medium was recovered from cultures at 40 h post-transfection, and virus in supernatant was concentrated using 10-kDa Amicon Ultra-15 centrifugal filter units (Millipore). Myoblasts were incubated with 1/10-concentrated supernatant and 8 μg/ml Polybrene in order to achieve 90 to 100% transduction efficiency. Because pLKO.1 shRNA plasmids contain a puromycin resistance gene, transduction efficiency was evaluated by puromycin selection. Cells were used for assays at 3 days postransduction.

For ectopic expression of myristoylated AKT (gift from Anthony Chi and Avinash Bhandoola), retroviral particles bearing migR expression plasmids were generated in HEK-293T cells as described above. Viral supernatant was concentrated, as described above, and administered to myoblasts. Myoblasts were transduced, as described above, with 1/10-concentrated supernatant in order to achieve 80 to 90% transduction efficiency. Because migR plasmids facilitate coexpression of green fluorescent protein (GFP), transduction efficiency was evaluated based on GFP positivity by immunofluorescence (IF). Cells were used for assays at 3 days postransduction.

siRNA transfection. For small interfering RNA (siRNA)-mediated knockdown of *Hif1α*, C2C12 cells were treated with siRNA duplexes (100 nM) according to the HiPerfect protocol (Qiagen) for 24 h. After 48 h, cells were changed to differentiation conditions. The following duplexes were used: HIF1α targeting siRNA H1 (SI00193011), HIF1α targeting siRNA H4 (SI00193032), and negative control siRNA (SI03650325).

Quantitative RT-PCR (qRT-PCR). Total RNA was isolated from cells using the TRIzol reagent protocol (Invitrogen) and from skeletal muscle tissue using the RNAeasy minikit (Qiagen). mRNA was reverse transcribed using the High-Capacity RNA-to-cDNA kit (Applied Biosystems). Transcript expression was evaluated by quantitative PCR of synthesized cDNA using an Applied Biosystems 7900HT sequence detection system. Target cDNA amplification was measured using TaqMan primer/probe sets (Applied Biosystems) for *Hif1α*, *Epas1*, *MyoD*, *Myogenin*, *Pgk1*, *Hey1*, *Hey2*, *HeyL*, *Hes1*, *Mxi1*, and *18S*.

Western blot analysis. Whole-cell and whole-tissue lysates were prepared in radioimmunoprecipitation assay (RIPA) buffer (150 mM NaCl–1% NP-40–50 mM Tris [pH 8.0]–0.1% SDS–0.5% Na-deoxycholate). Proteins were subsequently separated by SDS-PAGE and transferred to nitrocellulose membranes. Membranes were probed using the following antibodies: rabbit anti-HIF1α (Cayman), mouse anti-MYOD (Novus), mouse antimyogenin (Santa Cruz), rabbit anti-myogenin (Novus Biologicals), mouse anti-myosin heavy chain (anti-MHC; MF-20; DSHB), rabbit anti-β-tubulin (Cell Signaling), rabbit anti-poly(ADP-ribose) polymerase (anti-PARP; Cell Signaling), rabbit anti-AKT (Cell Signaling), rabbit anti-P-AKT S473 (Cell Signaling), rabbit anti-P-AKT T308 (Cell Signaling), rabbit anti-phosphorylated glycogen synthase kinase 3α/β S21/S9 (anti-P-GSK3α/β S21/S9; Cell Signaling), rabbit anti-GSK3β (Cell Signaling), rabbit anti-P-FOXO1/3A (Cell Signaling), rabbit anti-P-P70 S6K (Cell Signaling), rabbit anti-P70 S6K (Cell Signaling), rabbit anti-P-S6 S240/S244 (Cell Signaling), rabbit anti-S6 (Cell Signaling), rabbit anti-P-IGF-IRβ Y1135 (Cell Signaling), rabbit anti-IGF-IRβ (Cell Signaling), rabbit anti-P-IRS1 S636/S639 (Cell Signaling), rabbit anti-P-IRS1 S307 (Cell Signaling), rabbit anti-P-IRS1 S612 (Cell Signaling), rabbit anti-IRS1 (Cell Signaling), rabbit anti-IRS2 (Cell Signaling), rabbit anti-P-MEK1/2 S217/S221 (Cell Signaling), rabbit anti-MEK1/2 (Cell Signaling), rabbit anti-P-ERK1/2 T202/Y204 (Cell Signaling), rabbit anti-ERK1/2 (Cell Signaling), rabbit anti-PERK (Rockland), rabbit anti-XBP1 (Santa Cruz Biotechnology), rabbit anti-CHOP (Santa Cruz Biotechnology), and rabbit anti-P-RICTOR S1235 (Cell Signaling). Densitometry was performed using NIH ImageJ software. Representative Western blotting images of multiple independent experiments are presented below.

Femoral artery ligation (FAL) studies. In 8- to 12-week-old mice (maintained on a mixed B6;129 background), hind limb ischemia was induced by ligating the left femoral artery as previously described (40). Briefly, the femoral artery was exposed at the hip and separated from the

femoral vein and nerve. Silk suture was passed under the artery and tied to occlude it. Limb perfusion measurements were taken before surgery, immediately following surgery, and 48 h later using diffuse correlation spectroscopy (DCS) (40). DCS measurements were performed using a home-built instrument with two continuous-wave, long coherent 785-nm lasers (CrystaLaser Inc., Reno, NV) and eight avalanche photodiodes (Perkin-Elmer, Canada). Data collection was performed simultaneously in both limbs, via four detectors distributed symmetrically along one single source positioned at the center. This allowed for two source detector separations (0.5 and 1.0 cm) from both the top and bottom of the source position. In order to compare flow from the same region over the two different positions, we measured 3 different points along the bottom portion of the DCS probe, symmetrically positioned in each limb. In addition, mice were imaged before and immediately after surgery using a laser doppler imager (Moor Instruments, United Kingdom). Anesthetized mice were placed on a black background and scanned at a rate of 10 pixels/ms with the imager. Data collection and image generation were conducted using Moor LDI software. At 48 h after ligation, extensor digitorum longus muscles were harvested from the nonligated (right) and ligated (left) limb and homogenized into TRIzol for mRNA analysis or into RIPA buffer for protein analysis.

IF and microscopy. Myoblasts were cultured in 24-well dishes and differentiated. At the time of harvest, cells were fixed to wells with 4% paraformaldehyde. Immunostaining was performed for MHC (MF-20; DSHB) or HIF1α (Cayman) followed by fluorescein-linked secondary antibody treatment (Alexa Fluor 488 or Alexa Fluor 594; Invitrogen). Mounting medium with 4′,6-diamidino-2-phenylindole (DAPI; Vector Labs) was applied last. Cells were imaged at 20× magnification (or 60× magnification for HIF1α staining) using an Olympus IX81 inverted fluorescence microscope. For differentiation assays, 4 to 5 fields (containing 900 to 1,200 nuclei per field) were analyzed per group/condition. For HIF1α staining, 4 to 5 fields (containing approximately 300 nuclei per field) were analyzed per group/condition. Image analysis was then performed using MetaMorph software to quantify total $DAPI^+$ nuclei, the $DAPI^+$ nuclei in MHC^+ cells, or the $HIF1\alpha^+/DAPI^+$ nuclei in a given field. To measure the degree of myoblast differentiation (or MHC^+ "myotube" formation), a fusion index was calculated: the number of $DAPI^+$ nuclei in MHC^+ cells in a field was divided by the total number of $DAPI^+$ nuclei in that same field. A ratio was generated for each field in an experimental group, and an average ratio was determined. To evaluate HIF1α positivity, the number of $HIF1\alpha^+/DAPI^+$ nuclei were quantified per field. The average number of nuclei per field was generated for each experimental group. After image analysis and data collection were complete, fluorescence images were processed (i.e., brightness/contrast enhancement/cropping) using Microsoft Office Picture Manager for manuscript preparation, ensuring that changes were applied equivalently to all parts of the image and to both experimental and control images.

RESULTS

Hypoxia inhibits primary and immortalized myoblast differentiation *in vitro*. To evaluate the impact of O_2 availability on muscle progenitor differentiation, we used established cell culture models of skeletal muscle development: the C2C12 murine myoblast cell line and primary adult mouse myoblasts. Myoblasts can be stimulated to terminally differentiate into multinucleated myotubes, signified by expression of MHC (56). The differentiation conditions recapitulated features of ischemia-induced muscle regeneration: reduced availability of serum factors and local compensatory induction of IGFs (17, 45, 56, 60, 61). Consistent with previous reports (15, 19, 25, 51, 64), culturing C2C12 cells under low-O_2 conditions (0.5%) caused a 95% decrease in the generation of MHC^+ myotubes after 96 h, compared to cells cultured at 21% O_2 ("normoxia") (Fig. 1B). Decreased MHC levels were confirmed by Western blot analysis over 3 days of differentiation (Fig. 1C). The decreased numbers of differentiated cells were not due to increased cell death, as exposure of C2C12 cells to 0.5% O_2 for 48 h did not affect PARP cleavage, a marker of apoptosis (2) (Fig. 1E). We also examined the expression of muscle regulatory factors MYOD and myogenin. During a 3-day time course, both mRNA and protein expression levels of MYOD and myogenin were reduced in myoblasts incubated at 0.5% O_2 (Fig. 1C and D), consistent with previous studies (15, 64). These data indicate that hypoxia inhibits the myogenic transcriptional program and terminal differentiation of C2C12 myoblasts.

We extended these analyses to primary skeletal myoblasts, obtained from the hind limb muscles of 8- to 12-week-old mice. We reproducibly found that differentiating primary adult skeletal myoblasts at 0.5% O_2 abrogated MHC^+ myocyte formation by IF and MHC protein levels by Western blotting (Fig. 1F and G). In addition, myogenin protein levels were also reduced in hypoxic myoblasts (Fig. 1G), in agreement with the studies of C2C12 myoblasts. Therefore, hypoxia negatively regulates the differentiation program of skeletal muscle progenitors in multiple systems.

Ischemia correlates with reduced MRF expression *in vivo*. In mouse models of PAD, the femoral artery providing blood to the hind limb muscles is ligated, producing acute skeletal muscle injury (7, 24, 45). Skeletal muscle progenitors as well as damaged muscle fibers experience O_2 and nutrient deprivation before the formation of new blood vessels and terminally differentiated muscle (7, 24, 45). We hypothesized that following ligation, hypoxic stress in skeletal muscle impedes progenitor differentiation until the revascularization process has restored nutrient availability. To evaluate this possibility, we surgically occluded the left femoral artery in 8- to 12-week-old adult mice and followed limb perfusion using both laser doppler imaging and diffuse correlation spectroscopy (40). Blood flow within the ligated limb was significantly reduced immediately following surgery (Fig. 2A and B) and 48 h later ($n = 4$) (Fig. 2B). At 48 h after ligation, extensor digitorum longus (EDL) muscles were harvested from the ligated and nonligated limbs ($n = 13$). Consistent with previous reports on the skeletal muscle response to ischemia (8), HIF1α protein expression was induced in ischemic EDL muscle relative to muscle from the nonligated leg (Fig. 2C). mRNA expression of differentiation markers *MyoD* and *Myogenin* were also analyzed. The expression of these factors, which promote terminal progenitor differentiation (32, 34), was significantly decreased (57% and 71%, respectively) in ischemic skeletal muscle compared to nonischemic EDL (Fig. 2D). Myogenin protein levels were also reduced in ischemic muscle (Fig. 2E). These data suggest that ischemic stress negatively regulates the myogenic program *in vivo*, which correlates with the effects of hypoxia on myoblast differentiation *in vitro*.

Hypoxia inhibits myoblast differentiation through HIF1α-dependent and -independent mechanisms. Next, we employed multiple RNA interference (RNAi) approaches to determine whether O_2 regulates myoblast differentiation through a HIF-dependent mechanism. C2C12 myoblasts were depleted of HIF1α by using lentiviral shRNA and then differentiated at 21% O_2 or 0.5% O_2. Based on IF, HIF1α protein levels were significantly increased in control cells at 0.5% O_2 but were undetectable in *Hif1α* knockdown cells (Fig. 3A). HIF1α depletion was confirmed by qRT-PCR (Fig. 3B) and Western blot assays (Fig. 3C). After 24 h under hypoxic conditions, the HIF1α target gene *Phosphoglycerate kinase 1* (*Pgk1*) was induced 8.7-fold in

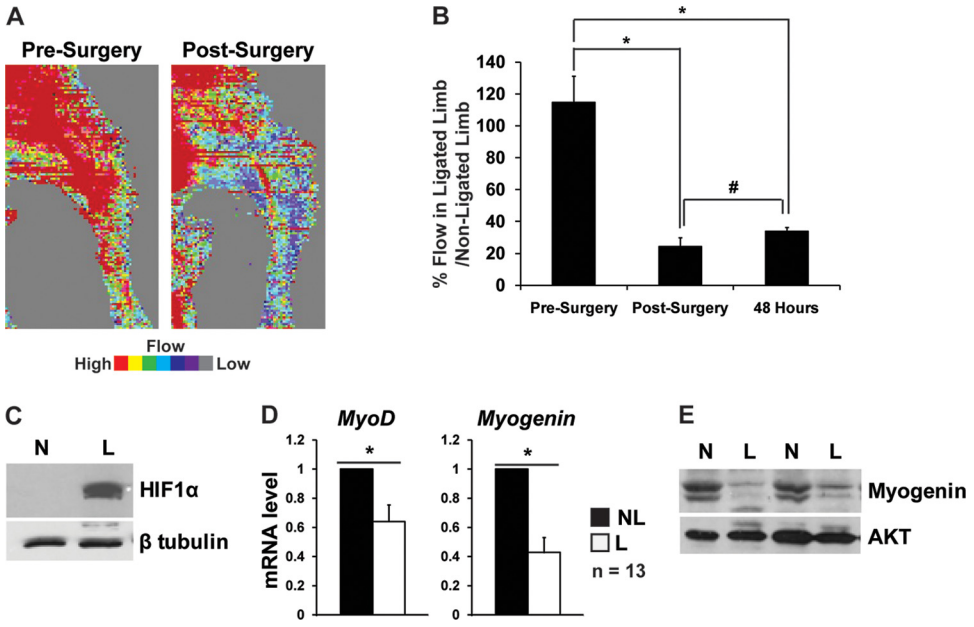

FIG 2 Skeletal muscle ischemia correlates with reduced MRF expression *in vivo*. (A) FAL was performed on 8- to 12-week-old mice. Limb perfusion was evaluated with a Moor laser doppler imager ($n = 11$) before surgery and immediately following surgery. Perfusion heat maps are displayed. (B) FAL was performed as described for panel A. Limb perfusion was evaluated by diffuse correlation spectroscopy immediately presurgery, immediately postsurgery, and at 48 h after ligation ($n = 4$). (C) HIF1α and β-tubulin protein expression levels were evaluated in EDL muscle lysates from nonligated (N) and ligated (L) limbs at 48 h after ligation. (D) *MyoD* and *Myogenin* mRNA levels were measured based on total RNA from EDL muscle of nonligated (NL) and ligated (L) limbs at 48 h after ligation ($n = 13$). (E) Myogenin and AKT protein expression levels were evaluated in EDL muscle lysates from nonligated (N) and ligated (L) limbs at 48 h after ligation. *, statistically significant difference based Student's *t* test ($P < 0.05$); #, not statistically significant different based on Student's *t* test ($P > 0.05$).

control cells but was not significantly changed in *Hif1α* shRNA-expressing cells (Fig. 3B).

We then evaluated expression of the myogenic program. Hypoxia repressed MYOD mRNA and protein levels independent of *Hif1α* shRNA expression (Fig. 3B and C). Incubating either control or knockdown cells under low-O_2 conditions also caused a reduction in myogenin (Fig. 3B and C): 91% versus 87% at the mRNA level and 60% versus 49% at the protein level based on densitometry. However, it should be noted that HIF1α-depleted myoblasts showed significantly increased normoxic levels of myogenin transcript and protein (2.5-fold and 1.8-fold, respectively); these cells, when incubated under hypoxic conditions, also expressed myogenin protein at levels comparable to normoxic control cells (89% of control cells). Similar effects on myogenin were observed when we used multiple independent siRNAs targeting *Hif1α* (Fig. 3D), suggesting that O_2 affects the expression of MRFs through HIF1α-dependent and -independent mechanisms.

Terminal differentiation was also evaluated at 48 h. Reduced O_2 availability resulted in significantly decreased MHC protein expression in control and HIF1α-depleted cells (by 91% and 79%, respectively) (Fig. 3E); similarly, hypoxia significantly impaired MHC^+ tube formation by 78% in control and by 60% in knockdown cells (Fig. 3F). However, HIF1α deficiency led to a 1.5-fold increase in myotube generation under conditions of 21% O_2 and restored tube formation under hypoxia to 58% of normoxic control levels. Overall, these data indicate that while HIF1α plays a modest role in myoblast differentiation, O_2 availability clearly modulates muscle progenitor differentiation through HIF1α-independent means as well.

We also considered if HIF2α compensated for HIF1α deficiency. Unlike HIF1α, HIF2α is expressed in select cell types and is regulated at the mRNA level (37). *Hif2α* mRNA levels were lower in C2C12 myoblasts and primary adult myoblasts (39-fold and 15-fold lower, respectively) than in primary macrophages, which normally express HIF2α protein (Fig. 3G). Also, both myoblast cell types exhibited lower *Hif2α* mRNA levels than mouse embryonic fibroblasts, which do not express detectable HIF2α protein (23). In contrast, *Hif1α* mRNA levels were comparable in all cell types examined (Fig. 3G). We conclude that *Hif2α* is expressed at very low levels in myoblasts, suggesting it plays a less important role in this lineage.

O_2 regulates myoblast differentiation independent of NOTCH. According to a prior study (25), hypoxia may regulate muscle progenitors through NOTCH signaling. We initially evaluated this model by measuring the effect of hypoxia on genes regulated by NOTCH transcriptional activity (27). Hypoxia induced the NOTCH target gene *Hey2*, consistent with a prior report (25), but not *Hey1*, *HeyL*, or *Hes1* in C2C12 cells (Fig. 4A).

As *Hey2* can be regulated through NOTCH-independent mechanisms (16), we assessed if hypoxic induction of *Hey2* requires NOTCH. We employed the NOTCH ligand JAG1 to activate signaling (35) as well as γ-secretase inhibitors (GSI) to suppress an essential enzyme in the pathway (30). An effective dose of the GSI DAPT (10 μM) was determined by evaluating its ability to suppress JAG1-dependent *Hey1* induction (Fig. 4B). Interestingly, we found that DAPT treatment did not significantly abrogate the hypoxic activation of *Hey2* (Fig. 4C), suggesting this effect is predominantly NOTCH independent. We also measured *Hey2* levels in response to combined hypoxia and JAG1 treatment. *Hey2* mRNA levels were promoted by JAG1 (6-fold) and hypoxia (33-

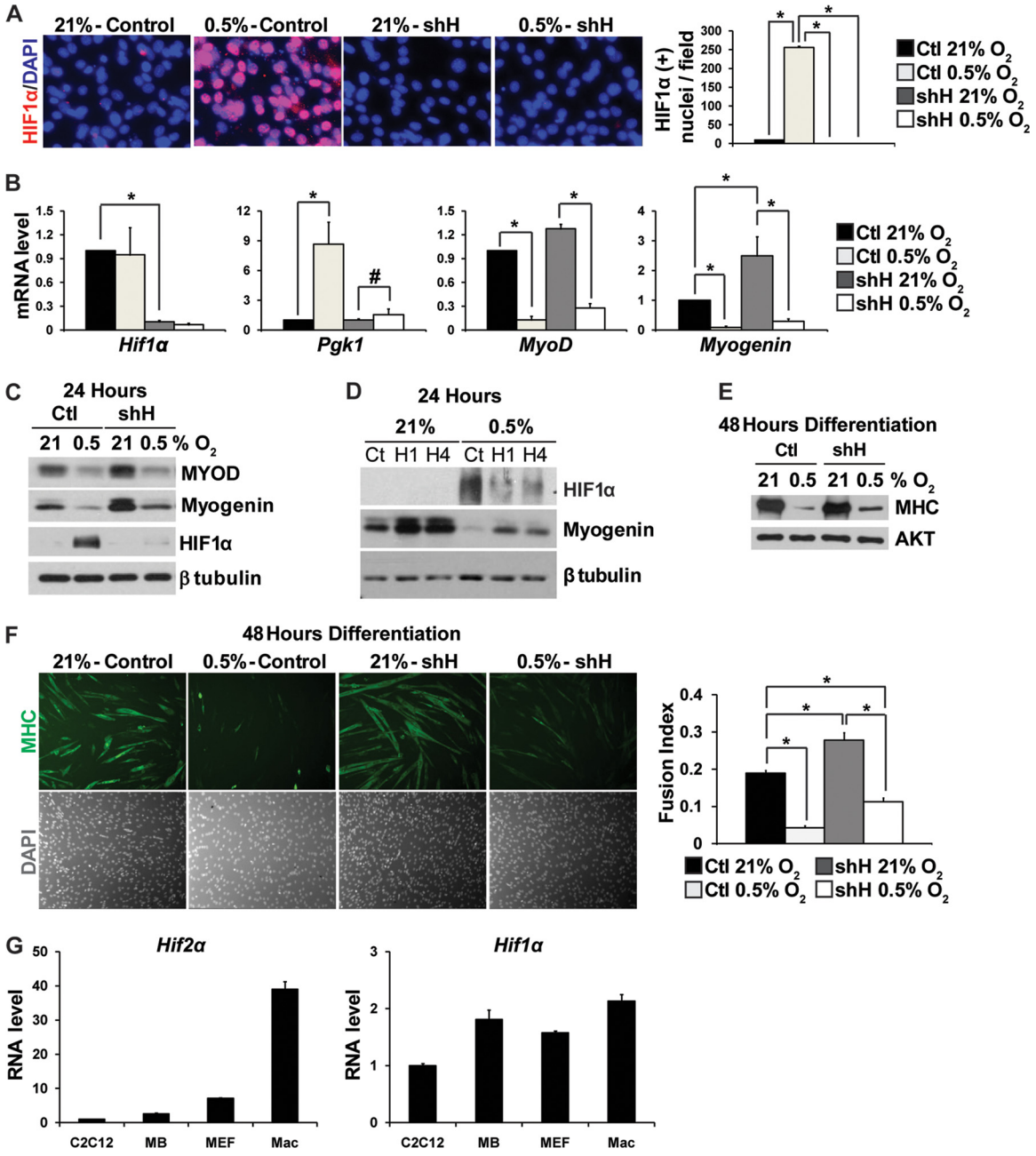

FIG 3 O_2 availability regulates skeletal myoblast differentiation through HIF1α-dependent and -independent mechanisms. (A) C2C12 myoblasts transduced with empty vector (Ctl) or *Hif1α*-targeting shRNA (shH) were differentiated for 24 h in 21% or 0.5% O_2. IF for HIF1α was performed. HIF1α$^+$ nuclear density was measured. (B) C2C12 cells were cultured as for panel A. *HIF1α*, *Pgk1*, *MyoD*, and *Myogenin* mRNA expression levels were determined. Averages of 3 independent experiments are shown. (C) C2C12 myoblasts were cultured as for panel A, and protein lysates were harvested. HIF1α, MYOD, myogenin, and β-tubulin protein levels were detected. (D) C2C12 cells were transfected with nonspecific siRNA (Ct) or two independent *Hif1α* siRNAs (H1 and H4) and differentiated for 24 h in 21% or 0.5% O_2. HIF1α, myogenin, and β-tubulin protein expression levels were measured. (E) C2C12 myoblasts transduced with empty vector (Ctl) or *Hif1α*-targeting shRNA (shH) were differentiated for 48 h in 21% or 0.5% O_2. MHC and AKT protein levels were evaluated. (F) C2C12 cells were cultured as described for panel E. IF for MHC was performed. The fusion index was calculated. (G) The mRNA expression levels of *Hif1α* and *Hif2α* were evaluated in C2C12 myoblasts, primary mouse myoblasts (MB), primary mouse embryonic fibroblasts (MEF), and primary mouse macrophages (Mac). *, statistically significant difference based on Student's *t* test ($P < 0.05$); #, not statistically significant difference based on Student's *t* test ($P > 0.05$).

fold), and the combination stimulated *Hey2* in an additive fashion (39-fold) (Fig. 4D). This suggests that NOTCH and O_2-sensing pathways do not synergistically regulate *Hey2* in myoblasts.

Hey2 appears to be less important for skeletal myogenesis than other NOTCH target genes (9). Therefore, we directly assessed whether NOTCH signaling contributes to hypoxic inhibition of myoblast differentiation. Myogenin protein expression, MHC protein levels, and MHC$^+$ tube formation were repressed at 0.5% O_2, independent of GSI treatment (Fig. 4E, F, and G). At 1% O_2—as used in a prior study (25)—MHC$^+$ tube formation was

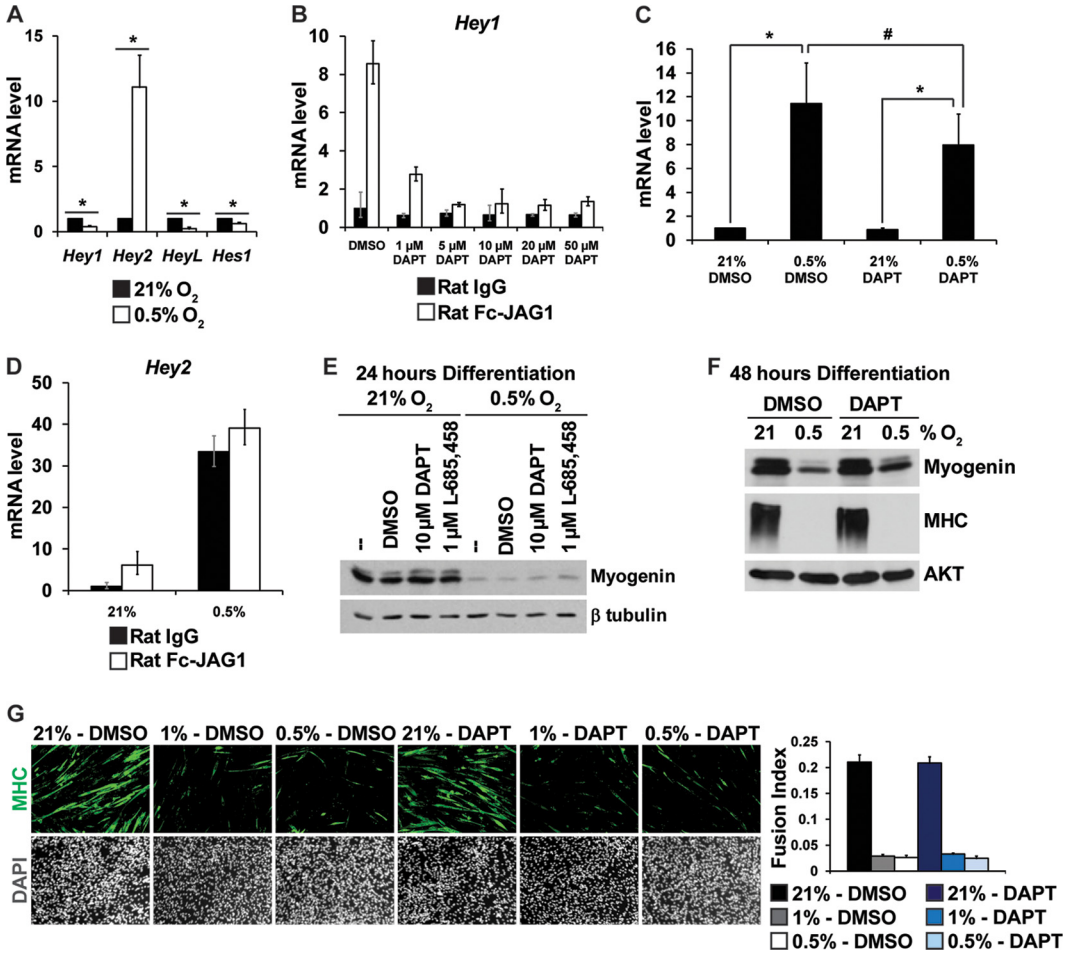

FIG 4 O_2 regulates myoblast differentiation independent of NOTCH. (A) mRNA levels of *Hey1*, *Hey2*, *HeyL*, and *Hes1* were measured in C2C12 myoblasts after 24 h of differentiation in 21% or 0.5% O_2. Averages of 3 independent experiments are shown. (B) *Hey1* mRNA expression was evaluated in C2C12 cells after 24 h exposure to Fc-JAG1 as well as various doses of the γ-secretase inhibitor DAPT. (C) *Hey2* levels were measured in C2C12 myoblasts after 24 h of differentiation in 21% or 0.5% O_2 with dimethyl sulfoxide (DMSO) or DAPT treatment. Averages of 5 independent experiments are shown. (D) *Hey2* levels were measured in C2C12 cells after 24 h of differentiation in 21% or 0.5% O_2 and on IgG or Fc-JAG1. (E) Myogenin and β-tubulin protein abundance levels were measured in C2C12 myoblasts after 24 h of differentiation in 21% or 0.5% O_2 with DMSO or two different GSIs, DAPT and L-658,458. (F) Myogenin, MHC, and β-tubulin protein levels were measured in C2C12 cells after 48 h of differentiation in 21% or 0.5% O_2 with DMSO or DAPT. (G) C2C12 myoblasts were differentiated for 48 h in 21%, 1%, or 0.5% O_2 and in either DMSO or DAPT. IF for MHC was performed. The fusion index was calculated. ∗, statistically significant difference based on Student's *t* test ($P < 0.05$); #, not statistically significant difference based on Student's *t* test ($P > 0.05$).

also repressed independently of GSI exposure (Fig. 4G). These results suggest that hypoxic effects on myoblast differentiation are NOTCH independent.

Hypoxia inhibits PI3K/AKT activity in a predominantly HIF1α-independent manner. Our data suggest that O_2 availability can regulate muscle progenitor differentiation through HIF-independent mechanisms. The PI3K/mTORC2/AKT pathway has been shown to promote myoblast differentiation *in vitro* and muscle development *in vivo* (13, 14, 28, 29, 41, 44, 47, 54, 59–62). Moreover, while AKT generates crucial responses to extracellular growth factors, this pathway is also sensitive to intracellular stress signals (12, 42, 43). We postulated that low O_2 availability blocks PI3K/mTORC2/AKT activity as a means of impeding differentiation. To assess this possibility, we measured levels of signal transduction downstream of PI3K (Fig. 5A).

Hypoxia repressed the phosphorylation of AKT at S473—a modification performed primarily by mTORC2 and required for maximal AKT activity (46)—over a 3-day differentiation time course (Fig. 5B). This effect was detectable within 12 to 16 h of O_2 deprivation (Fig. 5C). It was also observed at 1% O_2 (Fig. 5D), the O_2 tension used in a previous study that linked hypoxia to myoblast differentiation (25). Interestingly, incubating C2C12 myoblasts at 5% or 1.5% O_2 had modest effects on P-AKT S473 levels, indicating a threshold for AKT inactivation may exist between 1.5% and 1% O_2 (Fig. 5E). The phosphorylation of AKT at T308—mediated by 3-phosphoinositide-dependent kinase 1 (PDK1) and also essential for AKT activity (46)—was also diminished under hypoxic conditions (Fig. 5F), indicating that O_2 deprivation blocks multiple PI3K-dependent modifications of AKT.

In accordance with the less-active AKT, multiple direct substrates of AKT (38) exhibited decreased phosphorylation under low-O_2 conditions: GSK3α S21, GSK3β S9, FOXO3A T32, and FOXO1 T24 (Fig. 5G and H). AKT also indirectly promotes mTORC1 activity (38), and markers of mTORC1 signaling—P-

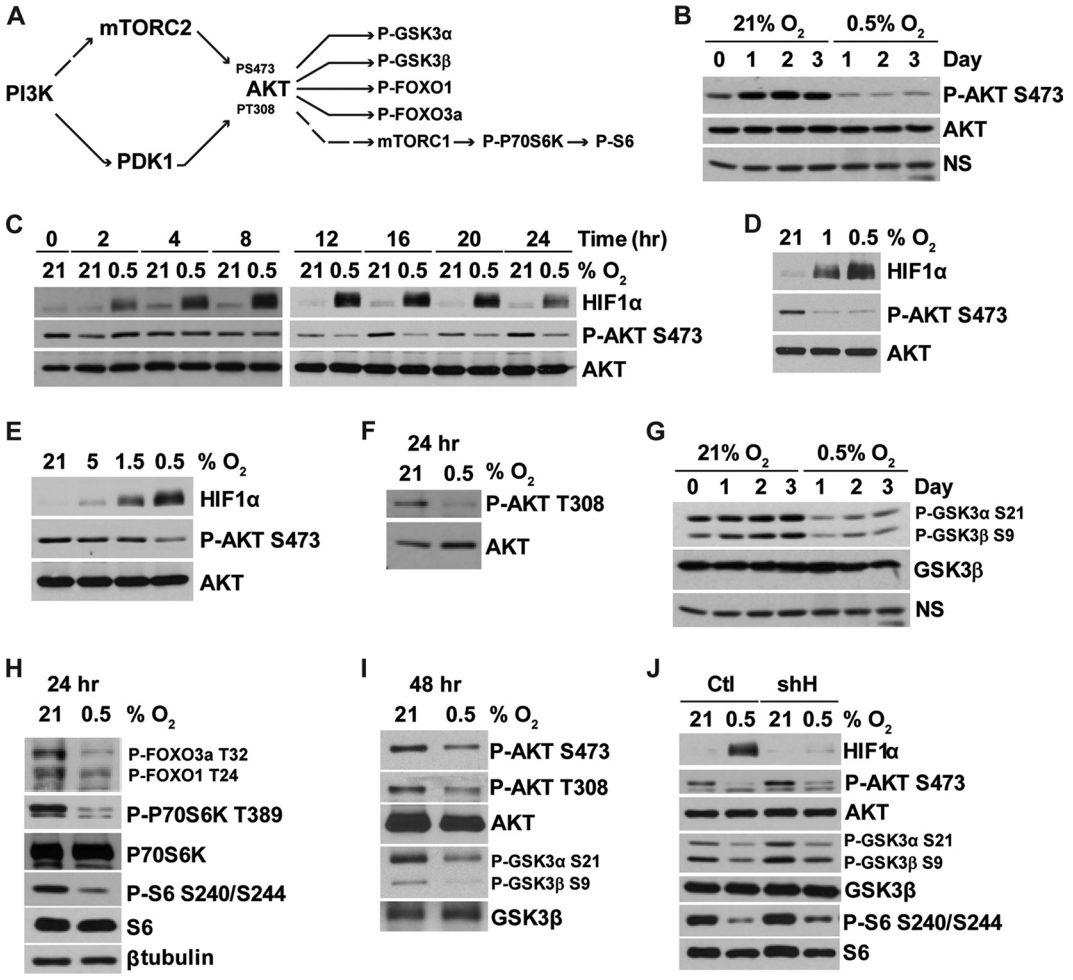

FIG 5 O_2 availability regulates PI3K/AKT pathway activity through a predominantly HIF1α-independent mechanism. (A) Model of the PI3K/AKT pathway. (B) P-AKT S473, AKT, and a nonspecific protein (NS) were detected in lysates of C2C12 myoblasts cultured with 21% or 0.5% O_2 for multiple days of differentiation. (C) C2C12 myoblasts were incubated at 21% or 0.5% O_2 under differentiation conditions. Cells were harvested at different times over 24 h for protein lysates. HIF1α, P-AKT S473, and AKT abundance levels were measured. (D) C2C12 cells were differentiated for 24 h with 21%, 1% and 0.5% O_2. HIF1α, P-AKT S473, and AKT expression levels were determined. (E) C2C12 cells were differentiated for 24 h at 21%, 5%, 1.5%, and 0.5% O_2. HIF1α, P-AKT S473, and AKT expression levels were determined. (F) C2C12 cells were cultured for 24 h under differentiating conditions at 21% or 0.5% O_2. P-AKT T308 and AKT expression levels were evaluated from protein lysates. (G) C2C12 cells were cultured as described for panel B, and lysates were probed for P-GSK3α S21/P-GSK3β S9, GSK3β, and a nonspecific band (NS). (H) C2C12 myoblasts were cultured as described for panel F. Levels of P-FOXO3A T32/P-FOXO1 T24, P-P70S6K T389, P70S6K, P-S6 S240/S244, S6, and β-tubulin were measured. (I) Protein expression levels of P-AKT S473, P-AKT T308, AKT, P-GSK3α S21/P-GSK3β S9, and GSK3β were detected from lysates derived from primary myoblast cultures after 48 h of differentiation at 21% or 0.5% O_2. (J) C2C12 myoblasts were transduced with empty vector (Ctl) or *Hif1*α shRNA (shH) and differentiated for 24 h at 21% or 0.5% O_2. The protein expression levels of HIF1α, P-AKT S473, AKT, P-GSK3α S21/P-GSK3β S9, GSK3β, P-S6 S240/S244, and S6 were measured by Western blotting.

70S6K T389 and P-S6 240/244—were similarly decreased under hypoxic conditions (Fig. 5H). These results indicate that O_2 affects AKT activity toward a broad group of substrates. We next examined if AKT signaling was sensitive to O_2 levels in primary myoblasts. Hypoxia caused a reduction in levels of P-AKT S473, P-AKT T308, P-GSK3α S21, and P-GSK3β S9 (Fig. 5I), consistent with reduced AKT signaling. This suggests that O_2 controls AKT activity in several models of muscle progenitor differentiation.

It remained unclear if these effects were HIF1α independent. HIF1α loss resulted in a modest induction of AKT activity at 21% O_2 (Fig. 5J), suggesting a role for basal HIF1α protein levels in restraining AKT. However, C2C12 cells expressing either empty vector or *Hif1*α shRNA exhibited similar reductions in AKT activity in response to hypoxia: P-AKT S473 (69% versus 66%), P-GSK3α S21 (65% versus 55%), P-GSK3β S9 (48% versus 43%), and P-S6 S240/244 (70% versus 54%) (Fig. 5J). This indicates that low O_2 levels inhibit PI3K/AKT activity in myoblasts through primarily HIF-independent pathways.

Inhibitors of PI3K and mTOR complexes mirror the effects of hypoxia on myoblast differentiation. To evaluate if O_2 regulates muscle differentiation through AKT, we compared the effects of O_2 deprivation and PI3K/mTORC2/AKT pathway inhibition on myogenesis. Multiple pharmacologic agents were employed, including rapamycin, which inhibits both mTORC1 and mTORC2 activity after prolonged exposure (52), and the PI3K inhibitor LY-294002. Treating differentiating myoblasts with either of these reagents or hypoxia resulted in similar decreases in P-AKT S473 and myogenin levels after 24 h (Fig. 6A). After 48 h,

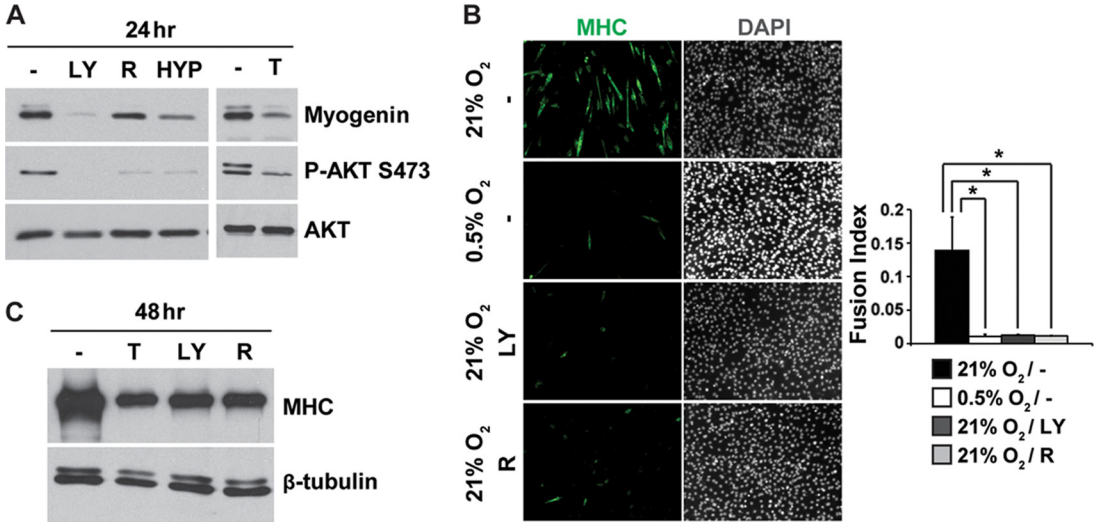

FIG 6 Inhibition of PI3K or mTORC activities mirrors the effects of hypoxia on myoblast differentiation. (A) C2C12 cells were differentiated for 24 h in the presenc or absence of PI3K inhibitor LY294002 (LY), mTORC inhibitor rapamycin (R), 0.5% O_2 (HYP), or mTORC inhibitor Torin1 (T). Myogenin, P-AKT S473, and AKT protein levels were determined. (B) C2C12 myoblasts were incubated for 48 h under the following conditions: no drug (21% O_2/-), low oxygen/no drug (0.5% O_2/-), PI3K kinase inhibitor LY294002 (21% O_2/LY), or mTORC inhibitor rapamycin (21% O_2/R). IF for MHC was performed. The fusion index was calculated. (C) C2C12 cells were differentiated for 48 h in the presence or absence of the PI3K inhibitor LY294002 (LY), mTORC inhibitor rapamycin (R), or mTORC inhibitor Torin1 (T). MHC and β-tubulin protein expression levels were assayed. *, statistically significant difference based on Student's *t* test ($P < 0.05$).

they also led to comparable reductions in MHC^+ myotube formation (Fig. 6B) and MHC protein levels by Western blot analysis (Fig. 6C). In addition, the more-specific ATP-competitive mTORC inhibitor Torin1 (58) yielded similar outcomes as rapamycin (Fig. 6A and C). In conclusion, inhibition of the PI3K/mTORC2/AKT pathway mirrors the effects of hypoxia on myoblast differentiation.

Derepression of PI3K/AKT activity in hypoxia restores myoblast differentiation. We then determined if derepression of PI3K/AKT signaling in hypoxia was sufficient to rescue muscle progenitor differentiation. First, we employed a myristoylated form of AKT (myrAKT) in order to restore AKT activity. AKT is normally recruited to the plasma membrane by the PI3K product phosphatidylinositol (3,4,5)-triphosphate (PIP3) (Fig. 7A) (11). This brings AKT into close proximity with its upstream kinase PDK1, promoting pathway activation (Fig. 7A) (11). In contrast, myrAKT does not require PIP3 for recruitment, because its myristoyl moiety docks myrAKT at the cell membrane. As a consequence, myrAKT is constituitively available for activation by PDK1. We observed that differentiating myoblasts transduced with myrAKT exhibited high levels of AKT activity irrespective of O_2 tension, in contrast to cells expressing the empty vector (Fig. 7B). After 48 h of differentiation, myrAKT expression was sufficient to markedly promote MHC^+ tube formation (Fig. 7C) and MHC levels (Fig. 7D), supporting the notion that AKT is a key driver of myoblast differentiation. In response to hypoxia, MHC^+ tube formation was only partially repressed in myrAKT-expressing cells relative to control cells (38% versus 96%) (Fig. 7C). Moreover, hypoxic C2C12 cells expressing myrAKT exhibited levels of MHC protein that were tantamount to normoxic control cells (Fig. 7D). These results indicate that elevating AKT activity through constituitive membrane recruitment is sufficient to restore myoblast differentiation in hypoxia.

We complemented these experiments with a second approach to restore PI3K/AKT activity in hypoxia: depletion of the lipid phosphatase and tensin homolog (PTEN). PI3K generates PIP3 from phosphatidylinositol (4,5)-bisphosphate on the inner leaflet of the plasma membrane, a reaction reversed by PTEN (Fig. 7A) (11). In turn, PIP3 molecules recruit PDK1 and AKT, drawing these factors into close proximity to one another and facilitating downstream signaling (Fig. 7A). PI3K activity and PIP3 have also been shown to enhance mTORC2 activity toward AKT (Fig. 7A) (11, 21). Reducing PTEN levels, therefore, should maintain PIP3 levels in the cell and promote AKT activity. We found that C2C12 cells lacking PTEN exhibited levels of PI3K/AKT activity under hypoxic conditions that were comparable to normoxic control cells (Fig. 7E). Moreover, phosphorylation of AKT effectors was impaired by hypoxia in control C2C12 cells but only modestly reduced in PTEN-deficient cells (Fig. 7E), including P-GSK3α S21 (51% reduction versus 10%), P-GSK3β S9 (50% versus 16%), and P-S6 S240/S244 (59% versus 23%). These effects are clearly important for differentiation, as PTEN inhibition in differentiating myoblasts restored MHC expression and MHC^+ tube formation under hypoxic conditions to levels reached by control cells under normoxic conditions (Fig. 7F and G). These experiments further support the notion that derepressing PI3K/AKT signaling under hypoxic conditions is sufficient to restore myoblast differentiation and suggest that O_2 regulates muscle progenitors through effects on this pathway.

O_2 availability influences IGF-I receptor sensitivity to growth factors. Finally, we determined how hypoxia blocks PI3K/AKT signaling in muscle progenitors, by considering several upstream points of regulation (Fig. 8A). Previous studies of cancer cells and fibroblasts have suggested that hypoxia can promote endoplasmic reticulum (ER) stress (63). Moreover, ER stress can negatively regulate PI3K/AKT signaling (12, 42, 43). Thus, we hypothesized that ER stress may facilitate AKT inactivation under low O_2 conditions. We evaluated several established markers (63)

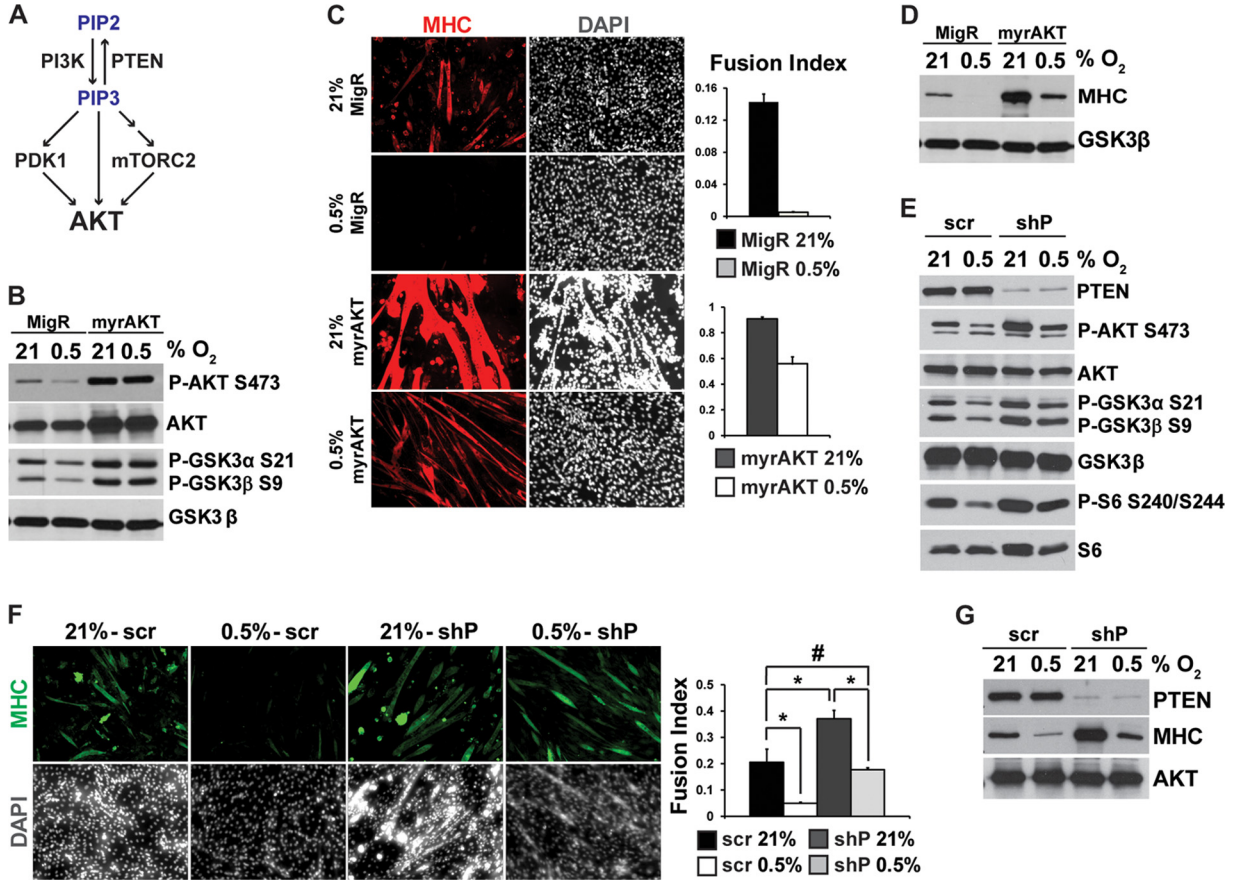

FIG 7 Derepression of PI3K/AKT signaling rescues differentiation under hypoxic conditions. (A) Model of phosphatidylinositol (3,4,5)-trisphosphate (PIP3) metabolism upstream of AKT. (B) C2C12 myoblasts were transduced with empty vector (MigR) or myristoylated AKT (myrAKT) and differentiated for 48 h at 21% or 0.5% O_2. P-AKT S473, AKT, P-GSK3α S21/P-GSK3β S9, and GSK3β protein levels were evaluated. (C) C2C12 myoblasts were cultured as described for panel B. IF for MHC was performed using Alexa Fluor 594-conjugated secondary antibody. The fusion index was calculated. (D) C2C12 myoblasts were cultured as described for panel B Protein expression levels of MHC and GSK3β were detected. (E) C2C12 myoblasts were transduced with scrambled shRNA (Ctl) or *Pten* shRNA (shP) and differentiated for 24 h at 21% or 0.5% O_2. Protein levels of PTEN, P-AKT S473, AKT, P-GSK3α S21/P-GSK3β S9, GSK3β, P-S6 S240/S244, and S6 were measured by Western blotting. (F) C2C12 myoblasts were transduced with scrambled shRNA (Ctl) or *Pten* shRNA (shP) and differentiated for 48 h under 21% or 0.5% O_2. IF for MHC was performed. The fusion index was calculated. (G) C2C12 myoblasts were cultured as described for panel F. Lysates were probed for PTEN, MHC, and AKT. *, statistically significant difference based on Student's *t* test ($P < 0.05$); #, not statistically significant difference based on Student's *t* test ($P > 0.05$).

of the ER stress response in hypoxic myoblasts: induction of phosphorylated PERK, spliced forms of XBP1, and CHOP. In the setting of ER stress, phosphorylated PERK migrates at a higher molecular weight on SDS-PAGE (6). However, incubating myoblasts at 0.5% O_2 for 24 h did not influence PERK levels or migration (Fig. 8B). In addition, the levels of unspliced XBP1, spliced XBP1, and CHOP were not changed after 24 h at 0.5% O_2, while P-AKT S473 was reduced as expected (Fig. 8B). This suggests that incubating differentiating myoblasts under hypoxia conditions did not alter ER stress levels above those observed under 21% O_2.

In addition, we examined two signals by which ER stress inactivates AKT (12, 42, 43). First, we evaluated the insulin receptor substrates 1 and 2 (IRS1 and IRS2), which link insulin/IGF receptors to downstream signaling components (38). In response to increased ER stress or negative feedback signals (e.g., from mTORC1), IRS can be destabilized through increased phosphorylation at crucial serine residues, leading to impaired AKT activity (38, 42, 43). However, in C2C12 cells cultured under low O_2 conditions for 24 h, we observed that IRS1 and IRS2 protein levels were unchanged and that serine residues in IRS1 were hypophosphorylated, suggesting these proteins were not destabilized in hypoxia (Fig. 8C). The reduction in phosphorylated IRS1 protein may instead reflect decreased mTORC1 activity (38, 43) (Fig. 5H). Second, we evaluated S1235 phosphorylation of mTORC2 component RICTOR, which is induced by ER stress and hinders the ability of mTORC2 to activate AKT (12). Phosphorylated and total RICTOR levels, however, were unchanged after 24 h at 0.5% O_2 (Fig. 8D). This suggests that hypoxia does not influence AKT through several ER stress-associated mechanisms.

Another regulator of PI3K/AKT signaling is the small GTPase RAS (11). In response to growth factors, RAS stimulates mitogen-activated protein kinases (i.e., MEK1/2, ERK1/2) and PI3K (11, 31). C2C12 myoblasts cultured under hypoxic conditions for 24 h exhibited normal levels of phosphorylated MEK1/2 and phosphorylated ERK1/2, the activated forms of these kinases (Fig. 8E). This suggests that hypoxia does not modulate AKT through effects on RAS and that O_2 affects select growth factor-dependent pathways in myoblasts.

We next evaluated whether IGF-I receptor (IGF-IR) expression or activity is regulated by O_2 availability, as this receptor

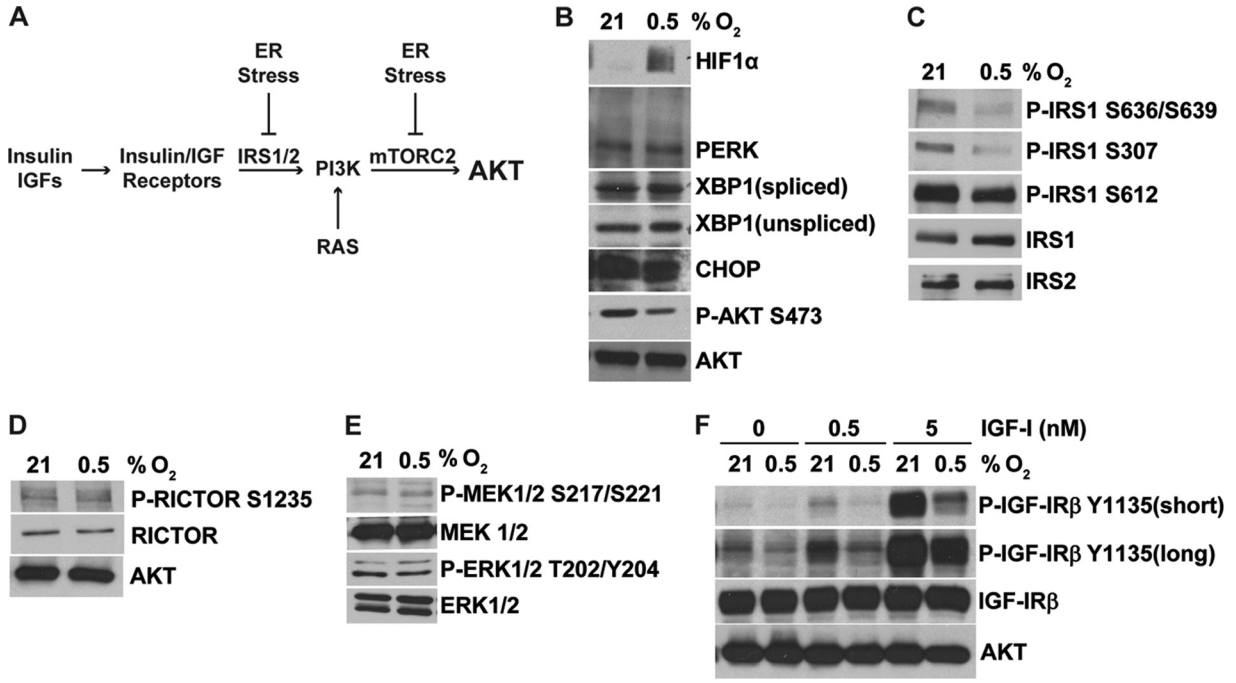

FIG 8 O_2 availability influences IGF-I receptor sensitivity to growth factors. (A) Model of IGF/insulin signaling upstream of PI3K/AKT. (B) C2C12 myoblasts were cultured for 24 h under differentiating conditions with 21% or 0.5% O_2. HIF1α, PERK, XBP1(spliced), XBP1(unspliced), CHOP, P-AKT S473, and AKT levels were quantified. (C) C2C12 myoblasts were cultured as described for panel B. P-IRS1 S636/S639, P-IRS1 S307, P-IRS1 S612, IRS1, and IRS2 protein levels were quantified. (D) C2C12 myoblasts were cultured as described for panel B. P-RICTOR S1235, RICTOR, and AKT protein levels were quantified. (E) C2C12 myoblasts were cultured as described for panel B. Expression levels of P-MEK1/2 S217/S221, MEK1/2, P-ERK1/2 T202/Y204, and ERK1/2 were assayed from myoblast protein lysates. (F) C2C12 myoblasts were cultured as described for panel B and pulsed with IGF-I. P-IGF-IRβ Y1135 (short and long exposures), IGF-IRβ, and AKT abundance levels were evaluated.

responds to endogenous IGFs and stimulates AKT activity during myoblast differentiation (60–62). C2C12 myoblasts were cultured under 21% or 0.5% O_2 for 24 h. Levels of phosphorylated IGF-I receptor β (P-IGF-IRβ)—the active form—were evaluated (Fig. 8F). While total IGF-IRβ was unaffected in 0.5% O_2, P-IGF-IRβ levels were reduced (Fig. 8F), indicating a smaller proportion of IGF-I receptors is active under hypoxic conditions. In addition, the cells were pulsed for 5 min with escalating doses of exogenous IGF-I, as this approach enabled us to measure the acute responsiveness of IGF-IRβ to growth factor. While IGF-I treatment promoted increased levels of P-IGF-IRβ under 21% O_2, this induction was blunted in hypoxic myoblasts (Fig. 8F). Total receptor levels were, again, unaffected (Fig. 8F). This indicates that hypoxia reduces the sensitivity of the IGF-I receptor to growth factors, providing a mechanism for how O_2 controls PI3K/AKT signaling in muscle progenitors.

DISCUSSION

Skeletal muscle stem/progenitor cells represent potential therapies for human skeletal muscle disease (22, 32, 34, 57). Determining what factors regulate these precursors will facilitate their use in muscle repair (22, 32, 34, 57). In the present study, we investigated how the differentiation of skeletal muscle progenitors is influenced by O_2 deprivation—a key feature of peripheral arterial disease (4, 7, 24, 26, 33, 45). We found that low O_2 inhibits terminal differentiation of both immortalized and primary myoblasts. Expression of the key muscle regulatory factors MYOD and myogenin is repressed by hypoxia *in vitro* and ischemia *in vivo*. To our surprise, hypoxia significantly modulates progenitor differentiation in the absence of HIF1α. We explored a HIF1α-independent role for O_2 in controlling PI3K/AKT signaling and concluded that low O_2 availability blocks this pathway as a means of impeding terminal differentiation.

Early reports linking O_2 to myoblasts did not evaluate if the HIFs were required for the effects of hypoxia (15, 25, 64). We observed that HIF1α loss has modest effects on myoblast differentiation at 21% O_2, consistent with a recent study (51). We also found that low O_2 levels significantly blocked progenitor differentiation in the absence of HIF1α expression. This implies that while HIF1α plays a modest role in myoblast differentiation, HIF-independent factors significantly regulate progenitor differentiation in response to hypoxia. These results were unexpected, for O_2 has been shown to control many developmental processes in a variety of lineages through HIF-dependent mechanisms (55). It suggests that O_2 may influence muscle development and regeneration *in vivo* through pathways other than HIF. Importantly, we have generated mice with targeted deletion of *Hif1α* or *Hif1β* in *Pax3*-expressing embryonic muscle progenitors, and skeletal muscle develops normally in these animals (data not shown).

We then evaluated which HIF1α-independent factors underlie the effects of low O_2 conditions. We focused on PI3K/AKT signaling, as this pathway is important in skeletal myogenesis (13, 14, 28, 29, 41, 44, 47, 54, 59–62). We observed that low O_2 levels blocked mTORC2-dependent phosphorylation of AKT and AKT-dependent activation of mTORC1 in C2C12 myoblasts. While this is consistent with a recent report (51), our study provides multiple

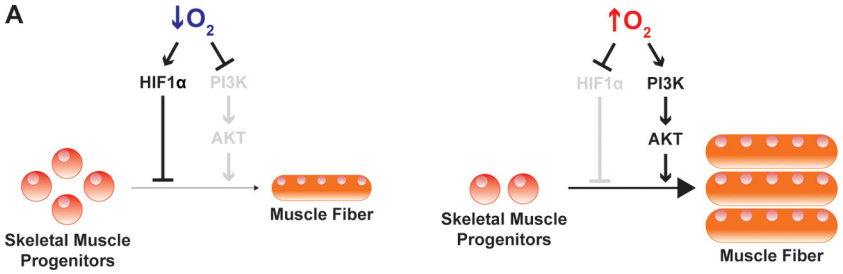

FIG 9 Model of O_2-dependent signaling in skeletal myoblasts. (A) At low O_2 levels ($\downarrow O_2$), progenitor differentiation is inhibited through induction of HIF1α and repression of PI3K/AKT signaling. When O_2 levels rise ($\uparrow O_2$), HIF1α protein levels diminish and AKT activity increases.

additional insights into O_2-dependent AKT inactivation. We showed that both PDK1- and mTORC2-dependent phosphorylation of AKT are repressed under hypoxic conditions. Moreover, we evaluated a wider array of AKT effectors beyond mTORC1, including GSK3α, GSK3β, FOXO3a, and FOXO1, and concluded that hypoxia broadly affects AKT activity. We also defined the kinetics and O_2 range for these effects and presented evidence that O_2-dependent regulation of AKT occurs in primary myoblasts. Myoblast differentiation was restored in hypoxia by derepressing not only AKT, as was previously shown (51), but also PI3K. In addition, we clarified the mechanism by which O_2 regulates AKT: reduced IGF-IR sensitivity.

Using lentivirus-mediated knockdown, we evaluated if hypoxic inactivation of AKT is HIF1α dependent. In contrast with the findings reported by Ren and colleagues (51), we observed that hypoxia regulates PI3K/AKT signaling in a predominantly HIF1α-independent fashion by using selected pools of knockdown cells as well as multiple monoclonal cell lines (data not shown). Unlike the previous report (51), we measured the ratio of phosphorylated AKT in 0.5% O_2 to levels in 21% O_2 for control and HIF1α knockdown cells, thereby evaluating how O_2 affects AKT in the presence or absence of HIF1α. We cannot exclude the possibility that a low level of HIF1α is sufficient to repress AKT activity under hypoxic conditions, although our lentivirus strategy reduced HIF1α levels by 90% uniformly across the transduced pool. Hence, it will be important in future studies to evaluate how O_2 regulates AKT in primary *Hif1α*-deleted myoblasts.

AKT inhibition was first detectable within 12 to 16 h of hypoxia exposure, suggesting that either a rapid posttranslational signal is not involved or sufficient time for turnover of an activated PI3K/AKT signaling component is needed. The latency of this response may also imply that O_2 affects this pathway through HIF-independent regulators of gene transcription (e.g., PGC1α) (37). In addition, we found that levels of phosphorylated AKT remained high under modest hypoxia (5% and 1.5%) but declined as O_2 concentrations decreased further (1% and 0.5%). This observation is consistent with previous reports in the literature suggesting that cells exert distinct hypoxic responses depending on the severity of O_2 deprivation (39). This sharp threshold suggests that the PI3K/AKT pathway may remain relatively active in skeletal muscle progenitors encountering mild hypoxia but would become impaired in more extreme O_2 deprivation during ischemic disease (4, 26, 33).

We also considered whether hypoxia suppresses AKT through increased ER stress (12, 42, 43, 63). In contrast to earlier studies performed in cancer cells and fibroblasts (63), myoblasts did not exhibit evidence of increased ER stress under hypoxic conditions, relative to levels under normoxic conditions. Moreover, several mechanisms of AKT inactivation associated with ER stress (12, 42, 43) were not engaged during hypoxia. These data suggest that ER sensitivity to hypoxic stress may depend heavily on cellular context and that ER stress does not mediate the observed inactivation of AKT.

Hypoxia is known to regulate mTORC1 through several mechanisms downstream of AKT, such as REDD1 induction and AMPK-dependent TSC1/2 activation (63). We observed that hypoxia suppressed mTORC1 signaling through AKT inactivation in myoblasts, as restoring PI3K/AKT activity in hypoxia (via *Pten* depletion) rescued mTORC1 activity. Hypoxic inactivation of AKT, therefore, represents an additional connection between O_2 and mTOR. In contrast to mTORC1, the regulation of mTORC2 is less well understood (53). Although hypoxia regulates mTORC2 activity in myoblasts, this is an indirect consequence of blunted IGF-IR signaling. Further investigation is required to determine how O_2 modulates receptor sensitivity (e.g., altered receptor localization or expression of a coreceptor) and if such mechanisms are engaged in other contexts.

Surprisingly, we observed that hypoxia regulates myoblast differentiation independent of NOTCH signaling. This differs from a past study linking HIF to NOTCH (25). In that report hypoxic conditions of 1% O_2 were used, while 0.5% O_2 was employed in most of the experiments in our study. Because exposure to these two O_2 levels could have distinct biological consequences (39), we compared their effects in several experiments. Both O_2 concentrations repressed "myotube" formation in a NOTCH-independent fashion, and AKT was sensitive to hypoxia at both O_2 tensions. This suggests that different hypoxic conditions do not account for our conflicting results. Nevertheless, our observations do not exclude the possibility that HIFs regulate NOTCH in other contexts (e.g., neural progenitors and thymic lymphomas) (5, 25).

The response of myoblasts to O_2 deprivation also appears to be distinct from that of cancer cells, where AKT signaling is unchanged or enhanced in response to hypoxia (1, 3). This may reflect a difference between normal and malignant cells, as tumor cells acquire genetic mutations (e.g., *PTEN* loss) that could maintain AKT activity in hypoxia and facilitate dysregulated growth.

To summarize, O_2 regulates skeletal muscle progenitor differentiation independently through HIF1α and PI3K/AKT signaling (Fig. 9A). We postulate that muscle stem/progenitor cells confronted with low O_2 availability (e.g., during ischemic injury) are maintained in an undifferentiated state, conserving these cells for appropriate circumstances for growth (Fig. 9A). Acute ischemia

may also repress muscle progenitor proliferation (data not shown). If neovascularization restores nutrient availability, muscle precursors can differentiate and contribute to new tissue (Fig. 9A). This model is supported by our observation that myogenic factors are decreased *in vivo* during acute ischemic stress. Because myofiber degeneration could partially account for this reduction, it will be important in future studies to evaluate if depletion of HIF1α and/or the O_2 sensor regulating PI3K/AKT can promote myogenic factor expression and myofiber regeneration in an ischemic injury model. This study, overall, provides new insights into how progenitors are regulated by their environment, and it has implications for skeletal muscle repair.

ACKNOWLEDGMENTS

We thank Jonathan Epstein, Mark Kahn, Gary Koretzky, Elisabeth Barton, Sarah Millar, Morris Birnbaum, Matt Buas, and Thomas Kadesch for helpful discussions during the formulation of these studies; Anthony Chi, Avinash Bhandoola, James Alwine, and David Sabatini for reagents; and Zachary Quinn and Theresa Richardson for technical assistance.

We report no conflicts of interest regarding this article.

We acknowledge funding support from NIH grant 5-R01-8L-066310. A.J.M. was supported through NIH training grant T32-AR053461-03 in Muscle Biology and Muscle Disease through the Pennsylvania Muscle Institute. M.C.S. is an investigator of the Howard Hughes Medical Institute.

REFERENCES

1. **Alvarez-Tejado M, et al.** 2001. Hypoxia induces the activation of the phosphatidylinositol 3-kinase/Akt cell survival pathway in PC12 cells. J. Biol. Chem. **276**:22368–22374.
2. **Amé J-C, Spenlehauer C, de Murcia G.** 2004. The PARP superfamily. Bioessays **26**:882–893.
3. **Arsham AM, Howell JJ, Simon MC.** 2003. A novel hypoxia-inducible factor-independent hypoxic response regulating mammalian target of rapamycin and its targets. J. Biol. Chem. **278**:29655–29660.
4. **Beckman JA, Creager MA, Libby P.** 2002. Diabetes and atherosclerosis. JAMA **287**:2570–2581.
5. **Bertout JA, et al.** 2009. Heterozygosity for hypoxia inducible factor 1α decreases the incidence of thymic lymphomas in a p53 mutant mouse model. Cancer Res. **69**:3213–3220.
6. **Bobrovnikova-Marjon E, et al.** 2008. PERK-dependent regulation of lipogenesis during mouse mammary gland development and adipocyte differentiation. Proc. Natl. Acad. Sci. U. S. A. **105**:16314–16319.
7. **Borselli C, et al.** 2010. Functional muscle regeneration with combined delivery of angiogenesis and myogenesis factors. Proc. Natl. Acad. Sci. U. S. A. **107**:3287–3292.
8. **Bosch-Marce M, et al.** 2007. Effects of aging and hypoxia-inducible factor-1 activity on angiogenic cell mobilization and recovery of perfusion after limb ischemia. Circ. Res. **101**:1310–1318.
9. **Buas MF, Kabak S, Kadesch T.** 2010. The Notch effector Hey1 associates with myogenic target genes to repress myogenesis. J. Biol. Chem. **285**:1249–1258.
10. **Bushby K, et al.** 2010. Diagnosis and management of Duchenne muscular dystrophy, part 1: diagnosis, and pharmacological and psychosocial management. Lancet Neurol. **9**:77–93.
11. **Cantley LC.** 2002. The phosphoinositide 3-kinase pathway. Science **296**:1655–1657.
12. **Chen C-H, et al.** 2011. ER stress inhibits mTORC2 and Akt signaling through GSK-3β-mediated phosphorylation of Rictor. Sci. Signal. **4**:ra10.
13. **Conejo R, Valverde AM, Benito M, Lorenzo M.** 2001. Insulin produces myogenesis in C2C12 myoblasts by induction of NF-κB and downregulation of AP-1 activities. J. Cell. Physiol. **186**:82–94.
14. **Coolican SA, Samuel DS, Ewton DZ, McWade FJ, Florini JR.** 1997. The mitogenic and myogenic actions of insulin-like growth factors utilize distinct signaling pathways. J. Biol. Chem. **272**:6653–6662.
15. **Di Carlo A, et al.** 2004. Hypoxia inhibits myogenic differentiation through accelerated MyoD degradation. J. Biol. Chem. **279**:16332–16338.
16. **Doetzlhofer A, et al.** 2009. Hey2 regulation by FGF provides a Notch-independent mechanism for maintaining pillar cell fate in the organ of Corti. Dev. Cell **16**:58–69.
17. **Erbay E, Park I-H, Nuzzi PD, Schoenherr CJ, Chen J.** 2003. IGF-II transcription in skeletal myogenesis is controlled by mTOR and nutrients. J. Cell Biol. **163**:931–936.
18. **Florina J, Ewton D, Coolican S.** 1996. Growth hormone and the insulin-like growth factor system in myogenesis. Endocrine Rev. **17**:481–517.
19. **Fu J, Taubman MB.** 2010. Prolyl hydroxylase EGLN3 regulates skeletal myoblast differentiation through an NF-κB-dependent pathway. J. Biol. Chem. **285**:8927–8935.
20. **Fulco M, et al.** 2008. Glucose restriction inhibits skeletal myoblast differentiation by activating SIRT1 through AMPK-mediated regulation of Nampt. Dev. Cell **14**:661–673.
21. **Gan X, Wang J, Su B, Wu D.** 2011. Evidence for direct activation of mTORC2 kinase activity by phosphatidylinositol 3,4,5-triphosphate. J. Biol. Chem. **286**:10998–11002.
22. **Glass D, Roubenoff R.** 2010. Recent advances in the biology and therapy of muscle wasting. Ann. N. Y. Acad. Sci. **1211**:25–36.
23. **Gordan JD, Bertout JA, Hu C-J, Diehl JA, Simon MC.** 2007. HIF-2α promotes hypoxic cell proliferation by enhancing c-Myc transcriptional activity. Cancer Cell **11**:335–347.
24. **Greco S, et al.** 2009. Common micro-RNA signature in skeletal muscle damage and regeneration induced by Duchenne muscular dystrophy and acute ischemia. FASEB J. **23**:3335–3346.
25. **Gustafsson MV, et al.** 2005. Hypoxia requires Notch signaling to maintain the undifferentiated cell state. Dev. Cell **9**:617–628.
26. **Hiatt WR.** 2001. Medical treatment of peripheral arterial disease and claudication. N. Engl. J. Med. **344**:1608–1621.
27. **Iso T, Kedes L, Hamamori Y.** 2003. HES and HERP families: multiple effectors of the notch signaling pathway. J. Cell. Physiol. **194**:237–255.
28. **Jiang B-H, Aoki M, Zheng JZ, Li J, Vogt PK.** 1999. Myogenic signaling of phosphatidylinositol 3-kinase requires the serine-threonine kinase Akt/protein kinase B. Proc. Natl. Acad. Sci. U. S. A. **96**:2077–2081.
29. **Jiang B-H, Zheng JZ, Vogt PK.** 1998. An essential role of phosphatidylinositol 3-kinase in myogenic differentiation. Proc. Natl. Acad. Sci. U. S. A. **95**:14179–14183.
30. **Jorissen E, De Strooper B.** 2010. γ-Secretase and the intramembrane proteolysis of Notch, p. 201–230. *In* R Kopan (ed.), Notch signaling. Academic Press, San Diego, CA.
31. **Kolch W.** 2005. Coordinating ERK/MAPK signalling through scaffolds and inhibitors. Nat. Rev. Mol. Cell Biol. **6**:827–837.
32. **Kuang S, Gillespie MA, Rudnicki MA.** 2008. Niche regulation of muscle satellite cell self-renewal and differentiation. Cell Stem Cell **2**:22–31.
33. **Lau JF, Weinberg MD, Olin JW.** 2011. Peripheral artery disease. Part 1: clinical evaluation and noninvasive diagnosis. Nat. Rev. Cardiol. **8**:429–441.
34. **Le Grand F, Rudnicki MA.** 2007. Skeletal muscle satellite cells and adult myogenesis. Curr. Opin. Cell Biol. **19**:628–633.
35. **Lindsell CE, Shawber CJ, Boulter J, Weinmaster G.** 1995. Jagged: a mammalian ligand that activates Notch1. Cell **80**:909–917.
36. **Liu J-P, Baker J, Perkins AS, Robertson EJ, Efstratiadis A.** 1993. Mice carrying null mutations of the genes encoding insulin-like growth factor I (Igf-1) and type 1 IGF receptor (Igf1r). Cell **75**:59–72.
37. **Majmundar AJ, Wong WJ, Simon MC.** 2010. Hypoxia-inducible factors and the response to hypoxic stress. Mol. Cell **40**:294–309.
38. **Manning BD, Cantley LC.** 2007. AKT/PKB signaling: navigating downstream. Cell **129**:1261–1274.
39. **Mansfield KD, et al.** 2005. Mitochondrial dysfunction resulting from loss of cytochrome c impairs cellular oxygen sensing and hypoxic HIF-α activation. Cell. Metab. **1**:393–399.
40. **Mesquita RC, et al.** 2010. Hemodynamic and metabolic diffuse optical monitoring in a mouse model of hindlimb ischemia. Biomed. Opt. Express **1**:1173–1187.
41. **Milasincic D, Calera M, Farmer S, Pilch P.** 1996. Stimulation of C2C12 myoblast growth by basic fibroblast growth factor and insulin-like growth factor 1 can occur via mitogen-activated protein kinase-dependent and -independent pathways. Mol. Cell. Biol. **16**:5964–5973.
42. **Özcan U, et al.** 2004. Endoplasmic reticulum stress links obesity, insulin action, and type 2 diabetes. Science **306**:457–461.
43. **Ozcan U, et al.** 2008. Loss of the tuberous sclerosis complex tumor suppressors triggers the unfolded protein response to regulate insulin signaling and apoptosis. Mol. Cell **29**:541–551.
44. **Pallafacchina G, Calabria E, Serrano AL, Kalhovde JM, Schiaffino S.**

2002. A protein kinase B-dependent and rapamycin-sensitive pathway controls skeletal muscle growth but not fiber type specification. Proc. Natl. Acad. Sci. U. S. A. **99**:9213–9218.
45. **Paoni NF, et al.** 2002. Time course of skeletal muscle repair and gene expression following acute hind limb ischemia in mice. Physiol. Genomics **11**:263–272.
46. **Pearce LR, Komander D, Alessi DR.** 2010. The nuts and bolts of AGC protein kinases. Nat. Rev. Mol. Cell Biol. **11**:9–22.
47. **Peng XD, et al.** 2003. Dwarfism, impaired skin development, skeletal muscle atrophy, delayed bone development, and impeded adipogenesis in mice lacking Akt1 and Akt2. Genes Dev. **17**:1352–1365.
48. **Philippou A, Halapas A, Maridaki M, Koutsilieris M.** 2007. Type I insulin-like growth factor receptor signaling in skeletal muscle regeneration and hypertrophy. J. Musculoskel. Neuron Interact. **7**:208–218.
49. **Provot S, et al.** 2007. Hif-1α regulates differentiation of limb bud mesenchyme and joint development. J. Cell Biol. **177**:451–464.
50. **Relaix F, Rocancourt D, Mansouri A, Buckingham M.** 2005. A Pax3/Pax7-dependent population of skeletal muscle progenitor cells. Nature **435**:948–953.
51. **Ren H, Accili D, Duan C.** 2010. Hypoxia converts the myogenic action of insulin-like growth factors into mitogenic action by differentially regulating multiple signaling pathways. Proc. Natl. Acad. Sci. U. S. A. **107**:5857–5862.
52. **Sarbassov DD, et al.** 2006. Prolonged rapamycin treatment inhibits mTORC2 assembly and Akt/PKB. Mol. Cell **22**:159–168.
53. **Sengupta S, Peterson TR, Sabatini DM.** 2010. Regulation of the mTOR complex 1 pathway by nutrients, growth factors, and stress. Mol. Cell **40**:310–322.
54. **Shu L, Houghton PJ.** 2009. The mTORC2 complex regulates terminal differentiation of C2C12 myoblasts. Mol. Cell. Biol. **29**:4691–4700.
55. **Simon MC, Keith B.** 2008. The role of oxygen availability in embryonic development and stem cell function. Nat. Rev. Mol. Cell Biol. **9**:285–296.
56. **Springer ML, Rando TA, Blau HM.** 2001. Gene delivery to muscle. John Wiley & Sons, Inc., Hoboken, NJ.
57. **Tedesco FS, Dellavalle A, Diaz-Manera J, Messina G, Cossu G.** 2010. Repairing skeletal muscle: regenerative potential of skeletal muscle stem cells. J. Clin. Invest. **120**:11–19.
58. **Thoreen CC, et al.** 2009. An ATP-competitive mammalian target of rapamycin inhibitor reveals rapamycin-resistant functions of mTORC1. J. Biol. Chem. **284**:8023–8032.
59. **Tureckova J, Wilson EM, Cappalonga JL, Rotwein P.** 2001. Insulin-like growth factor-mediated muscle differentiation. J. Biol. Chem. **276**:39264–39270.
60. **Wilson EM, Hsieh MM, Rotwein P.** 2003. Autocrine growth factor signaling by insulin-like growth factor-II mediates MyoD-stimulated myocyte maturation. J. Biol. Chem. **278**:41109–41113.
61. **Wilson EM, Rotwein P.** 2006. Control of MyoD function during initiation of muscle differentiation by an autocrine signaling pathway activated by insulin-like growth factor-II. J. Biol. Chem. **281**:29962–29971.
62. **Wilson EM, Rotwein P.** 2007. Selective control of skeletal muscle differentiation by Akt1. J. Biol. Chem. **282**:5106–5110.
63. **Wouters BG, Koritzinsky M.** 2008. Hypoxia signalling through mTOR and the unfolded protein response in cancer. Nat. Rev. Cancer **8**:851–864.
64. **Yun Z, Lin Q, Giaccia AJ.** 2005. Adaptive myogenesis under hypoxia. Mol. Cell. Biol. **25**:3040–3055.